NEPTUNE: OBSERVATIONS OF THE H_2 QUADRUPOLE LINES IN THE (4–0) BAND

L. TRAFTON

McDonald Observatory and Dept. of Astronomy, University of Texas at Austin, Tex., U.S.A.

Abstract. The first measurement of Neptune's quadrupole H_2 lines is reported. The equivalent widths of the S(0) and S(1) lines of the (4–0) band are given along with the corresponding widths measured from comparison spectra of Uranus taken on the same nights. These are interpreted in terms of both an inhomogeneous atmosphere overlying a reflecting layer and a homogeneous, semi-infinite, scattering atmosphere. Only the scattering model proves to be consistent with Neptune's spectrum in this wavelength region. The H_2 abundance along the scattering mean free path is found to be less than the value for Rayleigh scattering in pure H_2. This result is interpreted in terms of the presence of H_2, CH_4 and at least one other gas, instead of the more conventional interpretation in terms of the presence of an aerosol mixed with H_2. Weak features in the continuum were observed. Their widths and the strength of the H_2 features indicate that H_2 is more abundant than the sum of the remaining gases in these atmospheres.

1. Introduction

The only previous evidence that H_2 is a constituent of Neptune's atmosphere is the presence of the pressure-induced absorption feature of H_2 at $\lambda 8270$, first identified by Herzberg (1952). This feature is also present in the spectrum of Uranus but not in that of Jupiter or Saturn owing to greater aerosol scattering in their atmospheres. Quadrupole lines from both the (3–0) and (4–0) bands have been measured in the spectra of Jupiter and Saturn (see McElroy, 1969 for a review). Likewise, Uranus' quadrupole lines of the (4–0) band have been measured (Giver and Spinrad, 1966; Trafton, 1973; Price, 1973) as well as the quadrupole lines of the (3–0) band (Lutz, 1973; Trafton, 1973). Quadrupole H_2 observations were not accomplished for Neptune owing to the faintness of Neptune's spectrum.

This difficulty has resulted in very little data being obtained by means of which Uranus and Neptune might be differentiated. Consequently, it is commonly assumed that the atmospheres of these two planets are essentially alike. Nevertheless, there are indications that their spectra differ in some respects. For example, Wamstecker (1973) recently has found that Neptune's spectrum exhibits CH_4 bands which absorb more weakly in their central regions than do Uranus' bands. Neptune's geometric albedo also appears to be somewhat lower in the continuum than Uranus' is. Neptune's seasonal changes certainly cannot be as extreme as Uranus' since Neptune's equator is inclined only 29 deg to its orbital plane. As Uranus' axis moves towards the Sun during the next decade, the spectra of the two planets may become entirely different. Only observations of Neptune can establish Neptune's character; reliance should not be placed on any assumed similarity between these two planets.

I report herein the first detection of the quadrupole lines of H_2 in the spectrum of Neptune. The equivalent widths of the S(0) and S(1) lines of the (4–0) overtone band

Woszczyk and Iwaniszewska (eds.), Exploration of the Planetary System, 497–511.

of H_2 are presented along with their implications for the state of H_2 in Neptune's atmosphere. Particular attention is paid to differences between the H_2 spectra of Neptune and Uranus.

2. The Observations and Their Reduction

The observations of Neptune occurred during the months of May, June and July, 1973. Observations of Uranus were also acquired to serve as comparisons for Neptune and to facilitate setting up the spectrograph for the observations of Neptune. The dates and other observational conditions are given in Tables I and II for Neptune and Uranus, respectively. I employed the coudé scanner (Tull, 1972) of the 272 cm (107-in.) telescope of the McDonald Observatory, using an RCA 31034 photomultiplier having a GaAs photocathode and cooled by dry ice to yield a dark count of 1.5 s^{-1}. The spectrograph employed an echelle grating in a double-pass Littrow mode with a cross-dispersing grating to separate the overlapping orders. The spectrographic parameters are given in Table III.

The entrance slit width projected to 3.5″ on the sky so that it included practically all of Neptune's light. The signal was typically 11 s^{-1} for the S(0) line and 8 s^{-1} for the S(1) line. This difference arose largely because of the different settings with respect to the blaze of the echelle. Observational sessions of Neptune ranged from 2 to 6 h each. During an observation, 40 channels, each of width 50 mÅ or 46 mÅ for the S(0) or S(1) line, respectively, were sequentially scanned in each direction of the

TABLE I

Observations of Neptune

PLN #	Date	Scan cycles	Final airmass	Seeing (arc-sec)	Temp/ humidity (C/%)	Maximum counts/ch		Doppler shift	
						Net	Dark	(Å)	(ch)
				S(0) λ6435.0					
3616	17 May 73	5654	2.2	1	16/31	2650	429	−0.12	−2.3
3622	18 May 73	6722	1.7	1+	16/22	3225	510	−0.11	−2.1
3694[a]	10 Jun 73	3683	1.7	3	14/51	1288	369	+0.14	+2.9
3805	17 Jun 73	10767	4.1	1	23/15	5419	525	+0.22	+4.3
3832	18 Jun 73	9345	3.2	1–2	22/10	4574	456	+0.23	+4.5
				S(1) λ6367.7					
3563	10 May 73	5042	1.8	1	18/34	2330	262	−0.19	−3.8
3730	13 Jun 73	5288	3.5	2	16/45	1487	264	+0.18	+3.5
3749	15 Jun 73	7551	2.2	1½	21/30	3130	410	+0.20	+3.9
3767	16 Jun 73	5042	3.0	2–3	19/46	1700	260	+0.21	+4.1
3866	7 Jul 73	5648	2.4	1–3	21/21	1866	406	+0.40	+8.0
3943	8 Jul 73	4475	3.0	2–3	18/57	1487	250	+0.41	+8.2
3984	9 Jul 73	5061	3.0	2–3	18/52	1422	293	+0.42	+8.4

[a] Omitted from sums owing to cirrus and poor seeing.

https://doi.org/10.1017/S0074180900025742 Published online by Cambridge University Press

TABLE II

Comparison observations of Uranus

PLN #	Date	Scan cycles	Final hour angle	Seeing (arc-sec)	Temp/ humidity (C/%)	Maximum counts/ch		Doppler shift	
						Net	Dark	(Å)	(ch)
				S(0) λ6435.0					
3601	12 May 73	856	–	1	23/12	2507	75	+0.33	+ 7.1
3615	17 May 73	423	−0:16	1	16/24	1863	32	+0.36	+ 7.9
3620	18 May 73	2042	−1:46	1+	17/22	10305	153	+0.38	+ 8.2
3691	10 Jun 73	285	0:34	2	14/51	1142	40	+0.54	+11.8
3692	10 Jun 73	707	1:00	2	14/51	2719	100	+0.54	+11.8
3804	17 Jun 73	456	0:31	1	23/15	2399	27	+0.57	+12.4
3831	18 Jun 73	579	0:25	1	27/11	2961	39	+0.58	+12.6
				S(1) λ6367.7					
3729	13 Jun 73	521	2:26	2	16/45	1765	29	+0.55	+12.1
3748	15 Jun 73	323	0:40	1½	21/30	1250	10	+0.56	+12.3
3765	16 Jun 73	982	0:50	2−	22/40	2730	50	+0.57	+12.4
3865	7 Jul 73	354	2:42	1	21/28	1190	20	+0.62	+13.5
3942	8 Jul 73	387	3:49	2–3	19/55	1068	31	+0.62	+13.6
3983	9 Jul 73	452	3:12	2+	19/50	1218	32	+0.62	+13.6

TABLE III

Spectrographic parameters

Detector	RCA 31034 photomultiplier with GaAs photocathode
Dark count	1.5 s^{-1}
Gratings	Echelle, with 79 grooves mm^{-1} Cross disperser, with 300 grooves mm^{-1} blazed at 1 μ
Orders	
S(0)	35
S(1)	36
Filter	OG-515
Slit width	1500 μ
Resolution element	0.15 Å
Channel width	10 steps per channel
Step duration	2 ms

spectrum with a dwell time of 20 ms per channel. The scans were coadded and displayed in real time.

I divided the observed spectra by a white light spectrum in order to reduce the effect of vignetting in the spectrograph. A white light spectrum was obtained immediately after each observation of Neptune, without altering the spectrographic parameters, by scanning a ground glass screen placed before the entrance slit and illuminated by an incandescent source. This procedure was only partially successful in eliminating the vignetting because the ground glass screen illuminated more of the collimator than did the *f*/33 beam from the telescope. However, the residual slopes

of the continuum for the separate observations are in mutual agreement, including those of the comparison spectra taken of Uranus. These covered a wider bandpass, typically 60 channels, so they served the useful purpose of reducing the ambiguity in the residual slope of Neptune's continuum caused by weak features.

Because of the low signal, the individual observations of Neptune contained unacceptably high photon noise (as much as $\pm 3\%$ s.d.) for equivalent width measurements. To reduce this to acceptable values, I later summed the separate spectra obtained for a given line, shifting each in wavelength to account for the varying scan bandpass and Doppler shift. Summations of Neptune's spectra are shown in Figures 1 through 4. Figure 1 shows two partial summations of the S(0) line at

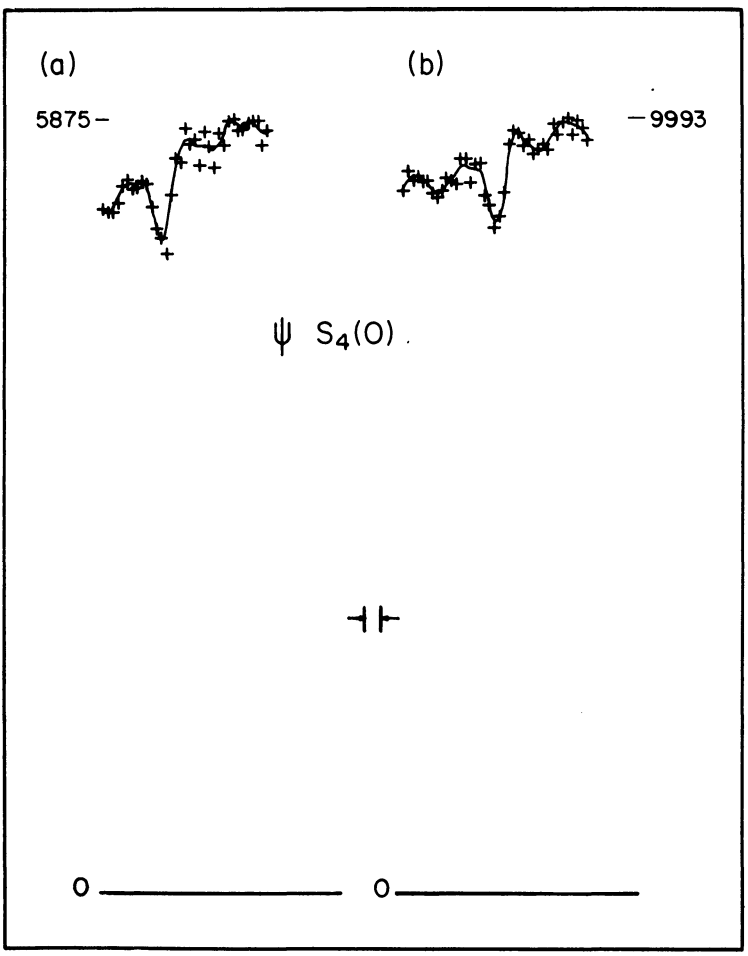

Fig. 1. Partial summations of Neptune's $S_4(0)$ H_2 line. The pluses denote the data and the continuous line is the optimally smoothed spectrum. The numbers indicate the maximum number of counts acquired per channel for each summation, respectively. (a) Summation of the May observations. (b) Summations of the June observations minus PLN ≠ 3694.

https://doi.org/10.1017/S0074180900025742 Published online by Cambridge University Press

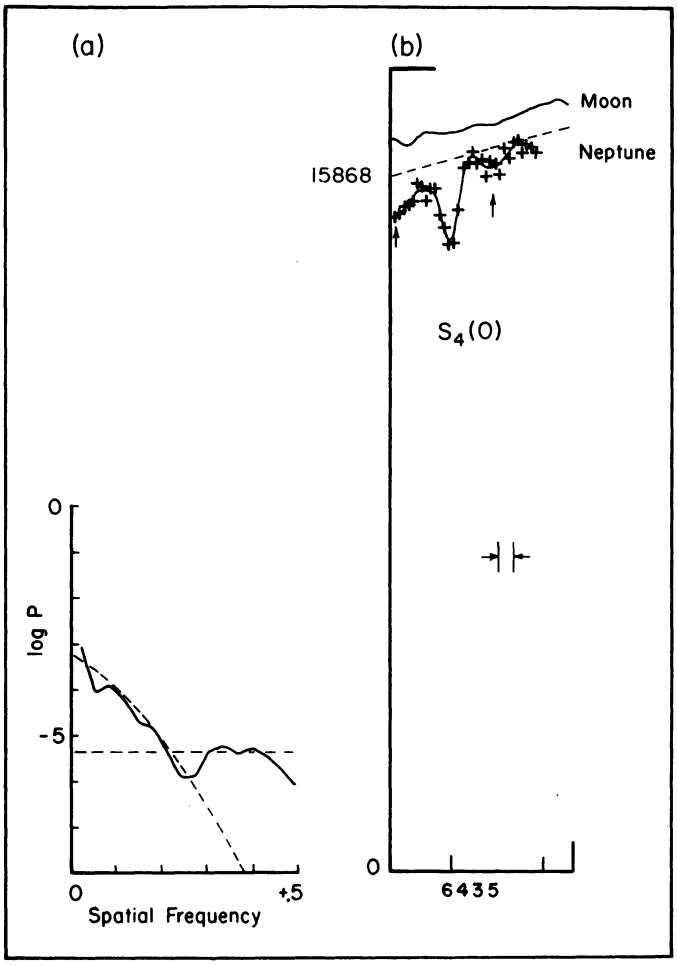

Fig. 2. (a) Power spectrum for the summation of Neptune's $S_4(0)$ H_2 line. The ordinate is the logarithm to base 10 of the spectral power and the abscissa runs from 0 to the Nyquist frequency. The dashed lines indicate a parabolic modelling of the signal part of the power spectrum and the whitenoise level. This model of the power spectrum determines the optimum smoothing. (b) Summations of Neptune's $S_4(0)$ H_2 line with Lunar comparison. The dashed line is the adopted continuum level; its slope was determined from wider spectra of Uranus. The pluses denote the data and the curve depicts the optimally smoothed spectrum. The vertical arrows mark the positions of weak features distinctly visible in the spectra of both Uranus and Neptune. The spectrographic resolution element is depicted schematically. The number is the maximum count acquired per channel and the scale is 20.0 ch $Å^{-1}$.

λ6435.0 for comparison and Figure 2 shows the summation of all the observations for S(0) except PLN# 3694, which was omitted owing to poor observing conditions. Figure 3 presents two partial summations for Neptune's S(1) line at λ6367.7 and Figure 4 gives the summation of all the observations of this line. Summations of the S(0) and S(1) lines in the spectra of Uranus are shown in Figure 5 for comparison with Neptune. The partial sums are entirely independent and so illustrate the effect

https://doi.org/10.1017/S0074180900025742 Published online by Cambridge University Press

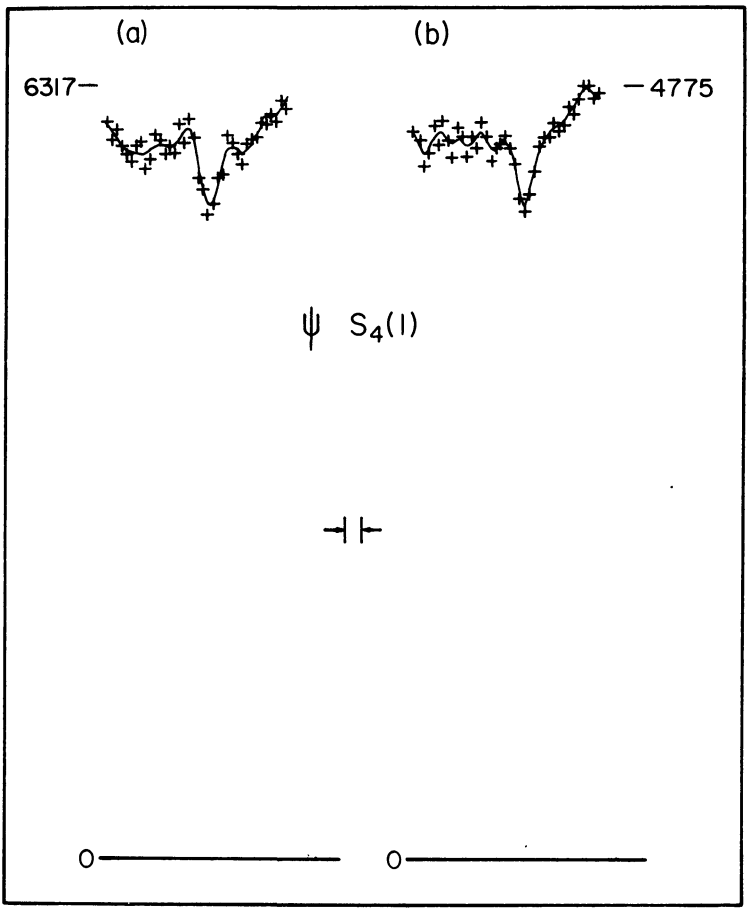

Fig. 3. Partial summations of Neptune's $S_4(1)$ H_2 line. The pluses denote the data and the continuous line is the optimally smoothed spectrum. The numbers indicate the maximum number of counts acquired per channe for each summation, respectively. (a) Summation of the June observations. (b) Summation of the July observations.

of photon noise and scintillation on the observations. The photon noise in the total sums is less than 1% since the total count is greater than 10^4 per channel.

Figures 3 and 4 also show lunar comparison spectra and the power spectra for the observations of Neptune. The power spectrum is a measure of the contribution that each frequency makes to the observed spectrum (cf. Bracewell, 1965) and is used to determine the optimum smoothing of the data. Following Brault and White (1971), I modelled the signal part of the power spectrum by a parabola and the noise part by a horizontal line corresponding to a white noise level. Each spectral frequency was weighted proportionally to the ratio of the signal power spectrum to the total power spectrum. The inverse transform then gives the optimally smoothed spectrum (Brault and White, 1971). The only subjective element in this smoothing arises from fitting

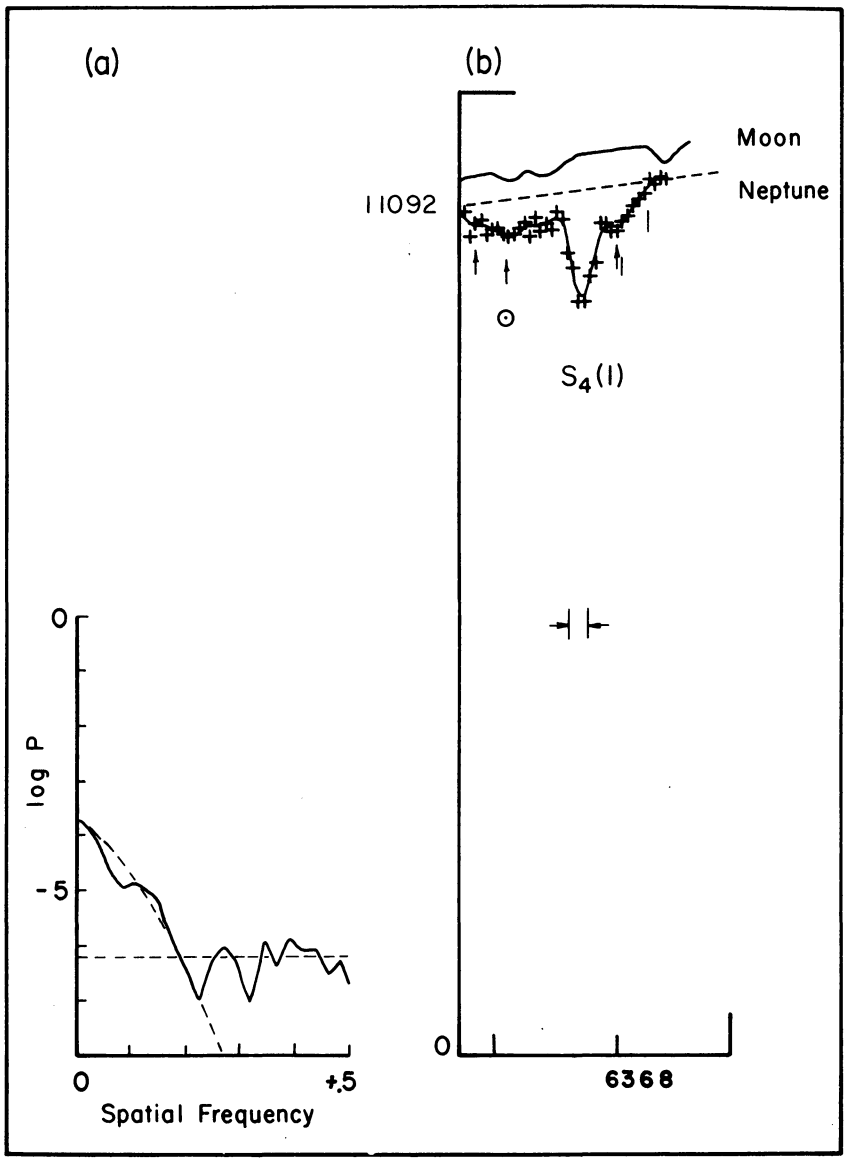

Fig. 4. (a) Power spectrum for the summation of Neptune's $S_4(1)$ H_2 line. The ordinate is the logarithm to base 10 of the spectral power and the abscissa runs from 0 to the Nyquist frequency. The dashed lines indicate a parabolic modelling of the signal part of the power spectrum and the white noise level. This model of the power spectrum determines the optimum smoothing. (b) Summations of Neptune's $S_4(1)$ H_2 line with lunar comparison. The dashed line is the adopted continuum level; its slope was determined from wider spectra of Uranus. The pluses denote the data and the curve depicts the optimally smoothed spectrum. The vertical arrows mark the positions of weak features distinctly visible in the spectrum of Uranus. The lines denote the location of a telluric H_2O feature occurring in Doppler shifted positions in Neptune's summation spectrum. This corresponds to the rightmost feature in the lunar spectrum. The symbol ○ indicates that a solar line may explain the corresponding mean absorption feature. The spectrographic resolution element is depicted schematically. The number is the maximum count acquired per channel and the scale is 21.9 ch $Å^{-1}$.

https://doi.org/10.1017/S0074180900025742 Published online by Cambridge University Press

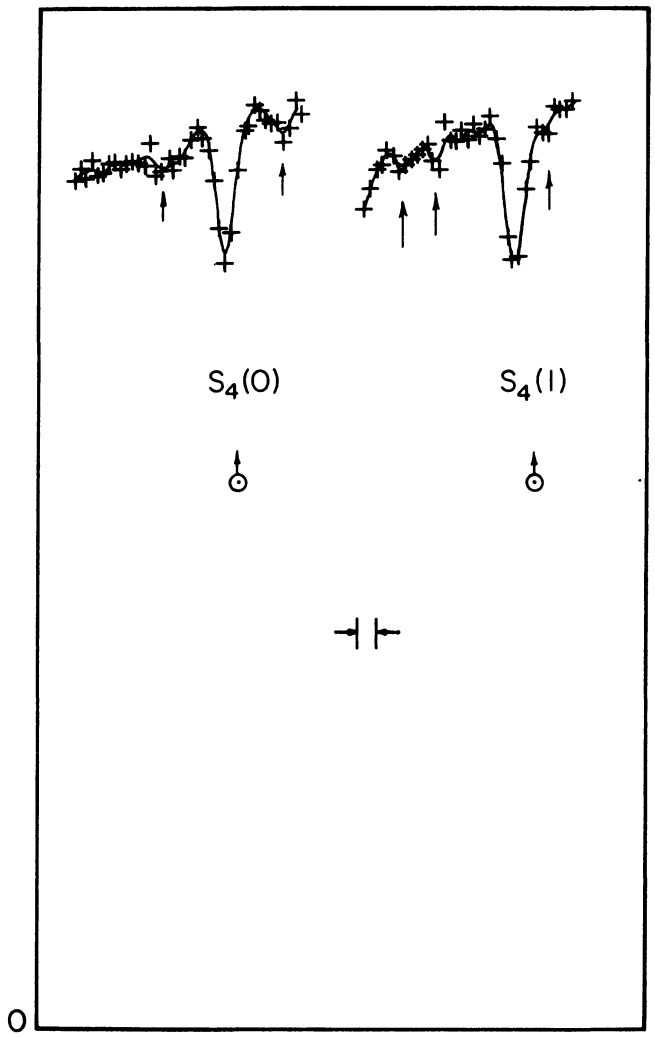

Fig. 5. Observations of Uranus' $S_4(0)$ and $S_4(1)$ H_2 quadrupole lines obtained for comparison with Neptune's spectra. The pluses denote the data and the curves are the optimally smoothed spectra. The arrows mark the positions of weak absorption features. The $S_4(0)$ line is PLN#3620 and has 10305 counts in its most highly filled channel. The $S_4(1)$ line is the summation of all the spectra obtained during the same nights as Neptune's $S_4(1)$ observations plus one more taken earlier. This summation has 10488 counts in its most highly filled channel. The standard deviation of the photon noise should be less than 1% of the continuum.

this model of the power spectrum to the actual one. Four points in the power spectrum must be chosen to effect the smoothing. The modelled power spectra are depicted in Figures 2a and 4a. The corresponding smoothed spectra are presented in Figures 2b and 4b. Note that the dispersion of the data points about their smoothed value is significantly reduced in the total summation of the observations for each line.

The greatest uncertainty in the measurement of the equivalent widths of the H_2 lines

https://doi.org/10.1017/S0074180900025742 Published online by Cambridge University Press

arises from the uncertainty in the location of the continuum rather than from the shape of the lines. Although the spectroscopic resolution element is 0.15 Å, there appears to be no region within the spectral bandpass of our observations which is sufficiently free of absorption features to permit establishing the continuum level accurately. The neighborhood of the S(0) line shows weak planetary features in both the spectra of Uranus and Neptune at +0.50 Å and −0.60 Å relative to the H_2 line. The S(1) line neighborhood shows features at −0.62 Å and −0.87 Å relative to the H_2 line and a blend at +0.27 Å in the wing of the Neptune H_2 line. The feature at −0.62 Å is probably the 2.5 mÅ solar feature at λ6367.13 and the blend is partly a telluric H_2O line at λ6368.46 and a weak planetary feature visible in the partial summation in Figure 3. Here, the Doppler shift clears the H_2O feature, revealing a weak absorption feature in the wing of the S(1) line. These features may be slightly stronger in the spectrum of Neptune.

The adopted continuum levels are depicted in Figures 2b and 4b where the slopes have been determined using the wider spectra of Uranus as discussed above. The equivalent widths were measured by approximating the shape of the H_2 lines by a triangle. The legs of the triangle were placed tangent to the line and the continuum

TABLE IV

Equivalent widths for H_2 lines in the (4–0) band

Neptune		Uranus comparisons	
S(0)	28 ± 4 mÅ	S(0)	29 ± 4 mÅ
S(1)	31 ± 4 mÅ	S(1)	33 ± 4 mÅ

level. Table IV gives the measured equivalent widths of Neptune's (4–0) H_2 features, as well as Uranus' for comparison. The uncertainties are estimated errors. Any systematic error resulting from the continuum placement would affect the spectra of both planets equally so that the relative measurements would still be meaningful.

3. Analysis

Upon comparing the spectra of Uranus and Neptune in Figures 2, 4 and 5, one notices that the H_2 lines in the spectra of Neptune are partially washed out with respect to their counterparts in the spectrum of Uranus. The lines are wider and their central intensities are greater. Their equivalent widths are only slightly less than the values measured for Uranus' features (refer to Table IV). Furthermore, the resolution of the weak features in the continuum appears to be similarly degraded in Neptune's spectrum. Since the pressure broadening coefficient of H_2 is small (0.0015 cm^{-1} atm^{-1} at room temperature) compared to that for CH_4, it appears unlikely that this could be simply a pressure effect. Pressures high enough to broaden significantly an H_2 spectral line of width 0.15 Å would wash out any weak CH_4 features.

Because of Doppler shifts arising from planetary rotation, one would expect the observed spectral resolution element to be larger than that corresponding to the slit width. Neptune's rotation period is $\frac{3}{2}$ of that for Uranus but Uranus' poles are inclined 57 deg to the line of sight while Neptune's is inclined much more. Furthermore, the observations of Uranus were made near the central meridian where at the coudé focus, only about 88% of Uranus' projected equatorial diameter entered the slit. These effects would reduce the Doppler broadening somewhat for Uranus.

The spectrograph itself can increase or decrease the resolution of spectra obtained from a rotating planet as the angle of the rotation axis with the slit is varied (Deeming and Trafton, 1970). For the June scans, Uranus' orientation favored an enhancement in the resolution. On the other hand, Neptune's orientation seldom was favorable because its axis rotated considerably with respect to the spectrographic slit during the long exposures. From these considerations, I estimate that the Doppler smearing of Uranus' features should be no more than 70% of the smearing for Neptune. The resulting Doppler shifts of the equatorial limbs of the two planets are 1.4 and 2.0 channels, respectively. Limb darkening and the circular geometry will weight the less Doppler shifted components more. In any case, the residual Doppler shift is less than 0.6 channel between the two planets. This appears to be less than the observed difference so that Neptune's spectral features may be intrinsically broader than Uranus' are, depending on the degree of possible enhancement of Uranus' spectral resolution.

The scan summations for both planets are slightly degraded in resolution owing to the change in Doppler shift with time and the constraint of allowing shifts of only integral channels in the summations. This should essentially affect the spectra of both planets equally since the number of spectra for each planet is about the same and a spectrum of each planet was obtained during a given night. This should not result in a spectral widening of more than one channel.

Since the entire disk of Neptune was included in the observations, it was necessary to average over the disk the equivalent width $W(\mu)$ calculated from models in order that theory may be compared with the observations. Here, μ is the direction cosine of the emergent radiation. The appropriate average is

$$\bar{W} = \frac{\int_0^\infty W(\mu)\, I(\mu)\, \mu\, d\mu}{\int_0^\infty I(\mu)\, \mu\, d\mu}.$$

For $I(\mu)$, I assumed the result for Uranus in the range $\lambda\lambda$3800–5800 obtained from Stratoscope II by Danielson *et al.* (1972).

I considered two extreme models for $W(\mu)$. The first is an inhomogeneous model consisting of a nonscattering gas overlying a reflecting layer. The structure of this model follows the calculations of Trafton (1967) and neglects all scattering. I have computed results for the inhomogeneous case for effective temperature 60 K since

measurements of Neptune's 20 μ flux by Morrison and Cruikshank (1973) indicate that Neptune's effective temperature may be as high as Uranus' is.

This model shows a curve of growth for the S(1) line which increases much more steeply than that for the S(0) line. The reason for this is that the state $J=1$ is sparsely populated in the upper layers of Neptune's atmosphere but becomes considerably more populated in the deeper layers. The population of the $J=0$ state, on the other hand, varies slowly over this range. This line is consequently less sensitive to the temperature structure. It implies an equilibrium H_2 abundance above the reflecting layer of 500 to 800 km-amagats, depending on the pressure. Other gases in the atmosphere would result in a lower H_2 abundance because they would increase the pressure.

The S(1) line is sensitive to the effective temperature of the model. For my $T_e=$ $=60$ K model, it implies an H_2 abundance of only 300 to 400 km-amagats for the same pressure range. Lowering the value of T_e would bring the ortho-para H_2 ratio closer to that for an equilibrium mixture, as would increasing the pressure by adding other gases.

The reflecting layer model is not appropriate for Neptune's atmosphere at these wavelengths because it implies quantities of gas so large that Rayleigh scattering cannot be ignored. The mean free path for light at these wavelengths is about 715 km-amagats H_2. My observations include the whole disk and would correspond to passage twice through the atmosphere. The observed strength of the $S(0)$ line then implies that most of the light would have been scattered. This result follows even for non-equilibrium ortho-para H_2 mixtures in Neptune's atmosphere. That scattering cannot be neglected in the formation of the (4–0) H_2 quadrupole lines is a conclusion Belton *et al.* (1971) came to regarding Uranus' spectrum.

Therefore, I considered the opposite extreme; namely, a homogeneous model consisting of a semi-infinite, isotropically scattering atmosphere (see, for example, Chamberlain, 1970). The results are analyzed in terms of the abundance of H_2 along a scattering mean free path (unit optical depth for scattering). I determined the continuum geometric albedo at this wavelength by measuring Neptune's spectral reflectivity with sufficient resolution to reveal the large-scale structure of the CH_4 bands and the interspersed continuum. The spectral reflectivity I derived by ratioing scans of Neptune to scans of the Moon and then correcting the result by the lunar reflectivity values obtained by McCord and Johnson (1970). The geometric albedos of Wamstecker (1973) at $\lambda 5000$ provided the necessary normalization to the spectral reflectivity scans. The continuum reflectivities between the CH_4 bands near $\lambda 6500$ fall nearly on a smooth curve so I used the value of this curve at $\lambda 6400$ to derive Neptune's geometric albedo in the continuum for the (4–0) H_2 lines. Assuming isotropic scattering, this leads to a single scattering particle albedo of 0.91. This value indicates that overlap from CH_4 lines is probably significant in the continuum.

Values of $\bar{W}$ were calculated from this model for a variety of temperatures and pressures. Figure 6 shows a self-consistent result giving 320 km-amagats of H_2 along a scattering mean free path for $W=28$ mÅ in the $S(0)$ line and $W=32$ mÅ in the $S(1)$ line. The corresponding temperature is 95 K and the effective pressure, P_e, is

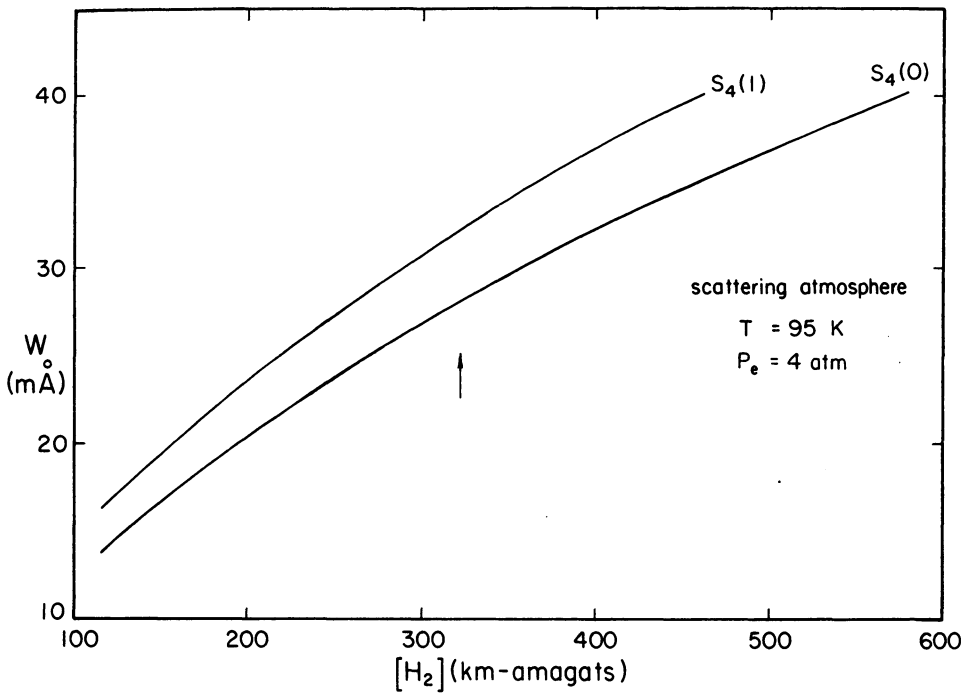

Fig. 6. Curves of growth for Neptune's (4–0) H_2 quadrupole lines. A semi-infinite, isotropically scattering atmosphere is employed, so the abscissa denotes the amount of H_2 along a scattering mean free path. To make the model consistent with the observations, a temperature of 95 K was chosen and an equilibrium distribution of ortho- and para H_2 was assumed. The results are for an effective pressure of 4 atm. The arrow indicates that a specific abundance of 320 km-amagats of H_2 is consistent with 28 mÅ and 32 mÅ for S(0) and S(1), respectively. The actual specific abundance of H_2 depends on the relative abundance and weight of the other gases in Neptune's atmosphere (see text).

4 atm. The value of the effective temperature is rather insensitive to P_e. This pressure is close to that which this quantity of H_2 would have at its base (3.2 atm) if arranged in a vertical column. Because of the inhomogeneous structure of the atmosphere and the random orientation of the scattering paths, the actual effective pressure may be less than this value, but this inference is uncertain because other gases may be present. For the physical conditions in this scattering model of Neptune's atmosphere, an increase in effective pressure results in an increase in $\bar{W}$. Therefore, the pressure broadening term dominates the collisionally narrowing term (cf. James, 1969) in the expression for the equivalent width. Reducing P_e by a factor of four increases the H_2 abundance along the scattering mean free path by only a factor of 1.39 when the absorption is held fixed. It is unlikely that the effective pressure is less than 1 atm because of the weight of the gas inferred from the observations and the isotropic character of the scattering. This minimum pressure sets a conservative upper bound of 450 km-amagats on the amount of H_2 in a mean free path, regardless of the model parameters.

Since the mean free path for Rayleigh scattering is 715 km-amagats H_2, the obser-

vations imply the existence of an aerosol or another gas in Neptune's atmosphere which reduces the scattering mean free path well below the Rayleigh scattering value for H_2.

It is unlikely that the effective pressure is much larger than about 3 atm because weak features in Neptune's spectrum are visible giving half-widths of about 6 channels, or a third of an ångström. If these arise from CH_4, their Lorentz width at 100 K can be estimated from the result Varanasi *et al.* (1973) obtain for the ν_3 band for CH_4 broadened by H_2, $\alpha_0 = 0.13 \pm 0.01$ cm^{-1} atm^{-1}. Using the relation $\alpha = \alpha_0 P_e$, where α is the half-width at half maximum, I estimate that $P_e \lesssim 2.8$ atm. For Uranus, $P_e \lesssim 1.9$ atm. If the continuum is higher, the width of the weak features would be greater and so also would the value of P_e. It is quite unlikely, however, that P_e exceeds twice this estimate.

4. Conclusions

Comparing Neptune with Uranus, the equivalent widths of the ortho- and para H_2 lines have about the same ratio in the spectra of the two planets. This is consistent with the notion of an equilibrium mixture of ortho- and para H_2 having the same temperature at the levels for which absorption effectively occurs in the scattering atmospheres of the two planets. The effective pressure may well be greater in Neptune's atmosphere since Neptune's surface gravity is 1.35 times greater. This would be consistent with the residual broadening of the weak features observed in Neptune's spectrum. In this case, the amount of H_2 in a scattering mean free path would be less in Neptune's atmosphere since the equivalent widths are comparable.

Since the geometric albedo of Neptune is less than Uranus' in this region of the spectrum (Wamstecker, 1973), the effective level of line formation may be higher in Neptune's atmosphere. If this is the case, the near equality in the rotational temperatures derived for these two planets would support the high effective temperature inferred from the measurements of Morrison and Cruikshank (1973). This reasoning depends on the steep scattering model for the atmospheres of these planets and the assumption that the relative strengths of the ortho- and para H_2 lines are determined by the local temperature.

Current thinking attaches any discrepancy between the equivalent widths of Uranus and those corresponding to a purely Rayleigh scattering atmosphere to the presence of an aerosol in the atmosphere (Belton *et al.*, 1971; Price, 1973). I find it odd that the density of any such aerosol would be just that giving a scattering mean free path within a factor of two or three of the Rayleigh value for pure H_2, particularly for both Uranus and Neptune. Aerosol densities several orders of magnitude higher or lower than this value might just as well occur. It seems much more likely that the observed H_2 abundance along the scattering mean free path results from the Rayleigh scattering in a *mixture* of H_2 with other gases in the atmospheres of these planets. In this case, no aerosol at all is required since the amount of H_2 along a mean free path is reduced when other gases are added. The mean free path itself is reduced since a photon may then be scattered by molecules other than H_2. Furthermore, since the ratio of H_2 to the remaining gases in these atmospheres is not likely to deviate more than an order

of magnitude from unity, a mixture would explain the narrow disparity between the observed H_2 specific abundances and that corresponding to Rayleigh scattering in pure H_2.

These two physical effects can be distinguished by observation since Rayleigh scattering varies with wavelength as λ^{-4} while aerosol scattering varies much more slowly. Furthermore, if other gases are responsible for the increased scattering, their weight would increase the effective pressure considerably while the aerosols have hardly any effect on the total pressure. The presence of other gases may alter the line broadening coefficient of H_2 and so affect the equivalent widths. Certainly, the increased pressure would reduce the estimates for the H_2 specific abundance since less H_2 would be required to produce the same absorption. This effect raises the estimate for the quantity of other gases along the scattering mean free path, and the resulting increased pressure feeds back to amplify this process. Convergence quickly occurs, though, since the optical depth from Rayleigh scattering along a mean free path is constrained to unity.

I have considered the effect of a number of gases in Neptune's atmosphere by neglecting their influence on the line broadening coefficient of H_2 but including their effect in broadening the H_2 lines as a result of increasing the total pressure. The amount of unknown gas required to give the observed H_2 equivalent widths depends on its mean molecular weight as well as on its refractive index and the amount of H_2.

This method is not effective for inferring the He/H_2 ratio because the Rayleigh scattering of He is 1/15 that of H_2. For example, if Neptune's equivalent widths are interpreted in terms of a H_2–He atmosphere having no aerosols, about 150 km-amagats of H_2 and 8800 km-amagats of He are required to give unit optical depth in Rayleigh scattering at $\lambda 6400$ and also to give the observed equivalent widths for the homogeneous scattering model at 95 K. The effective pressure is roughly approximated by half the weight of the gas in a mean free path when stacked in a vertical column. This yields an effective pressure of about 90 atm, a result clearly excluded by the observed widths of the weak features in the continuum. This means that any He in Neptune's atmosphere has a negligible effect on the scattering mean free path and can be ignored except for its effect on the total pressure.

A number of gases, such as A, N_2, O_2 and H_2O have very similar refractive indices; namely twice that of H_2. If these are lumped together with a designated mean molecular weight of 30, then they are compatible with the H_2 observations if there is 280 km-amagats of H_2 along the mean free path and 102 km-amagats of this unknown mixture. The resulting effective pressure would be about 8 atm. This pressure also appears to be higher than permitted by the widths of the weak features in Neptune's continuum. The conclusion must be that gases of these refractivities and molecular weights are not primarily responsible for the reduction in the mean free path from the Rayleigh scattering value in pure H_2.

The final category of other gases contains those gases having large refractive indices and low molecular weights. Prime examples are CH_4 and NH_3. To illustrate, a H_2–CH_4 atmosphere for Neptune would contain about 320 km-amagats of H_2 and

38 km-amagats of CH_4 along the scattering mean free path for an effective pressure of about 3 atm. This would correspond to a CH_4/H_2 ratio of about 0.12. This result is consistent with the observations and implies a rather high relative abundance of CH_4 compared to that in Jupiter or Saturn. However, the laboratory comparisons of Owen (1967) suggest smaller specific CH_4 abundances. Of course, other gases of high refractivity and low molecular weight may also be contributing to the reduction of Neptune's mean free path, in which case this abundance is characteristic of the sum of CH_4 and these unknown gases.

The major conclusion I draw from this analysis is that merely the visibility of weak features in the spectra of Uranus and Neptune indicates that H_2 must be more abundant than the sum of the other atmospheric constituents in these atmospheres because the spectra of these planets also imply large amounts of H_2 along the mean scattering paths. This result was previously suspected but until now lacked an observational basis. It contradicts an early deduction of Herzberg (1952), the basis of which has been recently questioned (cf. McElroy, 1969), that He should be more abundant than H_2 in these atmospheres. The second most abundant gas is likely to have a mixing ratio significantly smaller than unity. If an aerosol were responsible for the increased scattering, there would be no possibility of having gases other than H_2 and CH_4 present in the visible atmospheric regions in more than trace amounts.

Acknowledgements

It is a pleasure to acknowledge the assistance of J. Woodman in obtaining these observations. This research was supported as one phase of NASA Grant NGR 44-012-152.

References

Belton, M. J. S., McElroy, M. B., and Price, M. J.: 1971, *Astrophys. J.* **164**, 191.
Bracewell, R.: 1965, in *The Fourier Transform and Its Applications*, McGraw-Hill Book Co., New York, Chapter 6.
Brault, J. W. and White, O. R.: 1971, *Astron. Astrophys* **13**, 169.
Chamberlain, J. W.: 1970, *Astrophys. J.* **159**, 127.
Danielson, R., Tomasko, M., and Savage, B.: 1972, *Astrophys. J.* **178**, 887.
Deeming, T. J. and Trafton, L. M.: 1970, *Appl. Opt.* **10**, 382.
Giver, L. P. and Spinrad, H.: 1966, *Icarus* **5**, 586.
Herzberg, G.: 1952, *Astrophys. J.* **115**, 337.
James, T. C.: 1969, *J. Opt. Soc. Am.* **59**, 1602.
Lutz, B. L.: 1973, *Astrophys. J.* **182**, 989.
McCord, T. B. and Johnson, T. V.: 1970, *Science* **169**, 855.
McElroy, M. B.: 1969, *J. Atmospheric Sci.* **26**, 798.
Morrison, D. and Cruikshank, D. P.: 1973, *Astrophys. J.* **179**, 329.
Owen, T. C.: 1967, *Icarus* **6**, 108.
Price, M. J.: 1973, *Bull. Am. Astron. Soc.* **5**, 291.
Trafton, L. M.: 1967, *Astrophys. J.* **147**, 765.
Trafton, L. M.: 1973, *Bull. Am. Astron. Soc.* **5**, 290.
Tull, T. G.: 1972, in S. Laustsen and A. Reiz (eds.), *Proc. ESO/CERN Conference on Auxiliary Instrumentation for Large Telescopes*, Geneva, p. 259.
Varanasi, P., Sarangi, S., and Pugh, L.: 1973, *Astrophys. J.* **179**, 977.
Wamstecker, W.: 1973, *Astrophys. J.* **184**, 1007.